ACS APPLIED MATERIALS & INTERFACES

Research Article

www.acsami.org

Design of Stable and Powerful Nanobiocatalysts, Based on Enzyme Laccase Immobilized on Self-Assembled 3D Graphene/Polymer Composite Hydrogels

Nerea Ormategui,[†] Antonio Veloso,[†] Gracia Patricia Leal,[†] Susana Rodriguez-Couto,*[,‡,§] and Radmila Tomovska*[,†,§]

[†]POLYMAT and Departamento de Química Aplicada, Facultad de Ciencias Químicas, University of the Basque Country, UPV/EHU, Donostia-San Sebastián, Spain

[‡]CEIT, Unit of Environmental Engineering, Paseo Manuel de Lardizábal, Donostia-San Sebastián, Spain

[§]IKERBASQUE, Basque Foundation for Science, Bilbao, Spain

Supporting Information

ABSTRACT: Graphene-based materials appear as a suitable answer to the demand for novel nanostructured materials for effective nanobiocatalytic systems design. In this work, a design of stable and efficient nanobiocatalysts made of enzyme laccase immobilized on composite hydrogels [reduced graphene oxide (rGO)/polymer] is presented. The composite hydrogel supports were synthesized by self-assembly of graphene oxide nanoplatelets in the frame of a polymer latex matrix, where the polymer nanoparticles were adsorbed onto the GO surface, creating hybrid nanoplatelets. These hybrids self-assembled when ascorbic acid was added as a GO reducing agent and formed three-dimensional porous structures, greatly swollen with water, e.g., the composite hydrogels. The hydrogels were used as a support for covalent immobilization of the laccase. The performance of the nanobiocatalysts was tested in the oxidative degradation of the recalcitrant synthetic dye Remazol Brilliant Blue R in aqueous solutions. The biocatalysts showed strong dye discoloration ability and high stability as they preserved their catalytic action in four successive batches of dye degradation. The presented biocatalysts offer possibilities for overcoming the main disadvantages of the enzyme catalysts (fragile nature, high cost, and high loading of the enzyme), which would lead to a step forward toward their industrial application.

KEYWORDS: *graphene hydrogels, graphene 3D monoliths, porous monoliths, self-assembled graphene structures, laccase, nanobiocatalyst, Remazol Brilliant Blue R*

INTRODUCTION

Development of effective nanobiosystems on a thin interface between nano- and biotechnology is already a mature field of research. However, there are still intensive investigations in searching for novel nanostructured materials suitable to be combined with biologically active compounds. In this regard, the discovery of graphene with all its peculiar properties and multifunctionality has opened a completely new area of investigation within the field. Thus, for example, graphene has been widely used as a support to immobilize various enzymes for the development of nanobiocatalysts,[1,2] graphene hydrogels have been used as a support for the immobilization of the white-rot fungus *Trametes pubescens*,[3] graphene-based nanocomposite hydrogels have been employed for different biomedical applications,[4] etc. The suitability of graphene as a support comes from its two-dimensional (2D) or plateletlike structure that offers a large surface area accompanied by an incredible flexibility and excellent mechanical properties. While we recognize the tremendous interest in 2D structures, self-organized graphene-based three-dimensional (3D) macroporous structures are increasingly attracting the attention of the materials scientists, because of the significant increase in the amount of active material per projected area.[5] Despite this, the graphene supports have been used only in 2D form. 3D graphene-based hydrogels, in addition to their large surface area, contain large percentages of water trapped in the structure that implies an adequate aqueous environment for the enzymes. This is fundamental for preserving the active conformational structure of the enzymes and, hence, their catalytic activity.[6] 3D graphene networks can be obtained by self-assembly interactions of graphene oxide (GO) by reducing it back to hydrophobic graphene under heating or in the presence of

Received: April 17, 2015
Accepted: June 15, 2015
Published: June 15, 2015

DOI: 10.1021/acsami.5b03325
ACS Appl. Mater. Interfaces 2015, 7, 14104−14112

reducing agents, such as $NaHSO_3$, Na_2S, or ascorbic acid.[3,7,8] During the initial stages of reduction, the basal plane of graphene oxide is shifted from a hydrophilic state to a more hydrophobic regime, increasing significantly the interfacial energy in the dispersion. In attempts to decrease it, the platelets start to join in a spontaneous way forming 3D robust and porous structures, greatly swollen with water, e.g., graphene hydrogels.[3] The first encouraging results that we obtained were realized using those graphene hydrogels and their dried forms (i.e., xerogels) as supports for the immobilization of the white-rot fungus *T. pubescens*.[3] The immobilized microorganism on those graphene gels produced activities much higher than those obtained when using other inert supports, speaking about the possibility of a kind of synergy between the active compound and the support. Although we showed that the physical properties can be controlled by the synthesis conditions, the hydrogels were still quite difficult to handle. That is why in this work we reinforced the hydrogel by incorporating polymer nanoparticles into the structure. This strategy was expected to improve the consistency, durability, and mechanical properties of the graphene hydrogels.

To verify the support potential of those composite hydrogels, in this work the immobilization of the enzyme laccase was conducted. Such enzymes were obtained by cultivation of the fungus mentioned above (i.e., *T. pubescens*). Laccases (benzenediol:oxygen oxidoreductases, EC 1.10.3.2) are multicopper oxidases that are ubiquitous in nature and especially abundant in white-rot fungi. Laccase enzymes have been reported to have a wide variety of industrial and biotechnological applications.[9] Although the processes of laccase production have been improved in the past several decades, their industrial application is still hampered by the lack of long-term stability under storage and operational conditions and difficulties in the separation of laccases from the reaction systems. Immobilization of laccase on a suitable support can overcome those drawbacks by forming compact, robust, and stable nanobiocatalysts. Although thousands of supports and protocols for enzyme immobilization have been reported over the past 40 years, simple and efficient approaches (in terms of activity, stability, selectivity, and absence of inhibition) are lacking.[10,11] Therefore, the design of such a nanobiocatalyst with improved enzyme properties is still a challenging task.

In the recent literature, when graphene was mixed with inorganic nanoparticles[12] or polymers,[13−15] hybrid hydrogels with superior properties were formed, such as magnetism, photoelectricity, temperature sensitivity, and wastewater treatment.[12,16−18] Production of 3D hybrid graphene/polymer hydrogels was usually achieved via polymerization *in situ* of previously mixed graphene with monomers, reduced afterward.[15,19−21] However, the presence of toxic monomer residues in the hydrogel structure is not welcome, especially for bio-based applications, and a number of time-consuming purification steps are required, which complicate the procedures and make them more expensive and difficult to scale up. Therefore, the use of polymers as precursors for the synthesis of composite hydrogels becomes highly desirable, as they can be prepared in a controlled way, without being disturbed by the presence of graphene. Wang et al.[22] used a polymer precursor for the synthesis of a multifunctional hydrogel membrane by self-assembly of reduced GO (rGO) during filtration; however, their method is limited to the use of water-soluble polymers, which limits its application possibilities because of the mechanical property restrictions. Block polymer precursors for hybrid GO hydrogel synthesis were used for synthesis of composite hydrogels via a vacuum-assisted infusion process, followed by a hydrothermal method combined with freeze-drying by Liu et al.[23] Besides the complex procedure of synthesis, their method included two functionalization steps of the GO sheets, which make the procedure expensive and difficult to scale up. In the work presented here, a very simple, novel, and versatile method of composite polymer/graphene hydrogel synthesis is presented. The peculiarity of this method lies in the use of polymer latex (colloidally stable aqueous dispersion of polymer nanoparticles) as a matrix for the self-assembly process of the GO sheets. This allows a contact between the polymer nanoparticles and the GO nanoplatelets prior to reduction, which interact throughout supramolecular bonding and form hybrid particles, composed of graphene platelets decorated with polymer nanoparticles. These hybrid platelets during the reduction process with ascorbic acid are prone to organizing spontaneously into composite 3D porous structures, greatly swollen with water, e.g., graphene/polymer hydrogels.

Besides the simplicity, the presented method is environmentally friendly as water is used as a solvent in all phases of the synthesis and, thus, attractive for bio-based materials preparation. It is versatile, because a wide variety of different polymer nanoparticles can be used. Various functionalities can be introduced onto the polymer nanoparticles by functional monomers during the polymerization step that later can be used for tailored interactions with the graphene platelets or with the biologically active compounds. As a proof of concept, methyl methacrylate (MMA)/butyl acrylate (BA) copolymer latexes were used, in which two different copolymer compositions were investigated: 50/50 and 70/30 MMA/BA ratios. As poly(MMA) is a harder segment in the copolymer, by increasing its content, we expect to improve the mechanical properties of the hydrogels. Additionally, the polymer particles were functionalized with two different functionalities, Br and OH, to investigate their influence on the interaction of the polymer with the hydrogels and the interaction of the hydrogels with the biomolecule used in this study, i.e., the enzyme laccase. Finally, to the best of our knowledge, this is the first time these types of highly hydrophobic polymers were combined with graphene into a hydrogel structure.

The novel built nanobiocatalysts synthesized in the manner presented here were used to remove a synthetic dye from aqueous solutions. The nanobiocatalysts were shown to be incredibly stable, as they maintained their catalytic activity in four successive discoloration batches, with quite high synthetic dye concentrations. This supposes a step forward toward the commercial applications of laccases.

RESULTS AND DISCUSSION

Synthesis and Characterization of Graphene/Polymer Composite Hydrogels. When a GO dispersion was mixed with the latex, the polymer nanoparticles were allowed to interact with the platelets. The high concentration of oxygen-containing functional groups (OH, COOH, C═O, epoxy, etc.) on the GO platelets and their large surface area permitted the adsorption of polymer nanoparticles onto the platelets and the formation of hydrogen bonds between them. These hybrid GO/polymer nanoplatelets are composed of GO sheets decorated with polymer nanoparticles. After the addition of AsA at an increased temperature (90 °C), the reduction of GO started and a significant decrease in the number of oxygen

DOI: 10.1021/acsami.5b03325
ACS Appl. Mater. Interfaces 2015, 7, 14104−14112

functionalities on the GO surface occurred, leading to an increase in the hydrophobicity of the platelets. The interfacial energy in the dispersion became significant, leading to coagulation of the hybrid platelets that started to organize spontaneously into composite hydrogels. They have an aspect of 3D monoliths with porous structures, swollen with water. In this way, an introduction of polymer particles into the supramolecular 3D rGO structure occurred. Figure 1 represents the proposed procedure schematically.

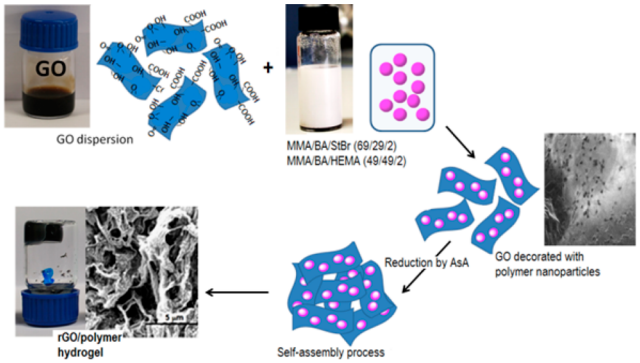

Figure 1. Synthesis procedure of composite hydrogels.

Incorporation of the polymer into the hydrogel structure is demonstrated by Fourier transform infrared (FTIR) spectra in Figure 2, where a comparison of the spectra of the neat

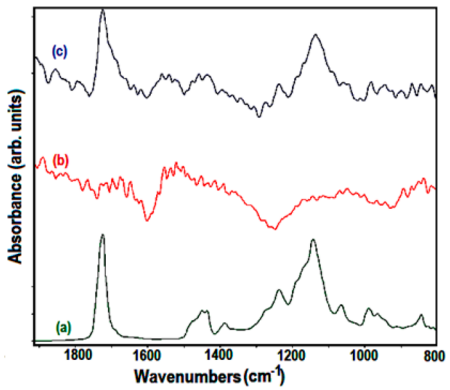

Figure 2. Comparison of the FTIR spectra of (a) neat polymer (70/30 MMA/BA weight ratio, Br-functionalized), (b) neat rGO, and (c) rGO/polymer composite hydrogel HG1.

polymer (Figure 2a) and the neat rGO (Figure 2b) with that of the composite hydrogel (Figure 2c) is presented. The presence of two pronounced stretching vibration bands in the spectra of the composite, corresponding to the carbonyl functionality (1720 cm^{-1}) and the C−O bond (1140 cm^{-1}), confirms the incorporation of the polymer into the self-assembled rGO structure.

As previously demonstrated,[3] the AsA plays an important role in the self-organization process, and with an increase in its amount, the properties of the hydrogels were improved. To determine if this was the case in the presence of the polymer, the amount of AsA was varied: the studied AsA/GO ratios were 0.5, 1, and 2 at a constant GO/polymer weight ratio of 1/1.8.

The consistency and mechanical properties of the gels improved continuously with the increased amount of AsA, although it was noticed that the polymer was not completely incorporated into the hydrogel structure. The values of the storage modulus, determined by dynamic rheology at 10 rad/s and 25 °C, were 12, 78, and 513 KPa for AsA/GO ratios of 0.5, 1, and 2, respectively. The value obtained for the largest AsA amount was approximately 1−3 orders of magnitude higher than those of conventional self-assembled polymers[24,25] or graphene-based composite hydrogels.[20,23] This significant improvement cannot be explained by the simple presence of AsA in the structure of the hydrogels. Keeping in mind the fact that these syntheses were performed in the presence of the same amount of polymer, we found that the amount of polymer incorporated into the structure likely depends on the pH of the latex matrix at different AsA contents.

It is well-known that the self-assembly processes of structures containing functionalities prone to H-bonding (such as carboxylic, for example) depend strongly on the pH of the solutions where they were performed.[26] Therefore, with a decrease in the latex pH, the charge state of the functional groups at the GO surface changes significantly. At the largest amount of AsA, most of the functional groups were protonated and promoted the formation of hydrogen bonding with the polymer chains, and thus, a larger amount of polymer was incorporated into the hydrogel structure, which, in turn, showed a higher mechanical strength.

The porous structure of the composite hydrogels is presented in Figure 3, where scanning electron microscopy (SEM) images of the hydrogel obtained with maximal AsA content are shown. In Figure 3a, under a lower magnification, a wide distribution of pore sizes ranging from 5 to ∼30 μm is presented. The same structure was apparent under a higher magnification (Figure 3b), in which besides the micropores, submicrometer pores are also presented. Figure 3b clearly illustrates rGO sheets decorated with a thin polymeric film. Figure 3c of the same sample, taken under high voltage and in high vacuum mode, reveals that the body of the hydrogel is made of one layer graphene 3D hollow structure (as a crumpled paper). To allow the incorporation of the whole amount of polymer from the latex, the procedure was slightly modified by increasing the contact time between the GO platelets and the polymer particles, and they were mixed for 3 h before the

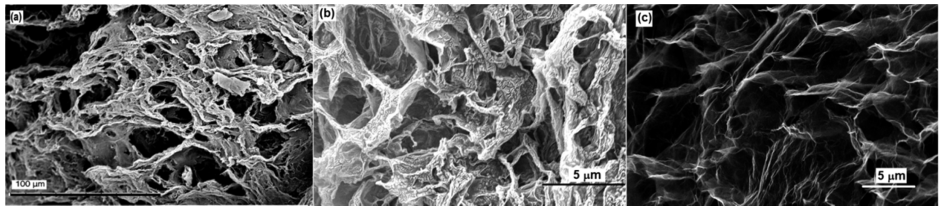

Figure 3. Morphology and structure of a HG3 hydrogel at (a) a lower magnification and (b and c) a higher magnification: (b) at a lower voltage and (c) at a high voltage in high-vacuum mode.

DOI: 10.1021/acsami.5b03325
ACS Appl. Mater. Interfaces 2015, 7, 14104−14112

reduction process. Two rGO/polymer weight ratios were investigated, 1/0.8 (HG1) and 1/2.4 (HG3), at a constant amount of AsA (AsA/GO ratio of 1). In addition, two different copolymer compositions and two different functionalities were used. The nanoparticles were functionalized with Br by using 2% functional monomer 4-bromostyrene (SBr) in relation to other monomers and with OH by using 1% 2-hydroxyethyl methacrylate (HEMA). The nomenclature of the hydrogels that will be used throughout this study is presented in Table 1, in relation to the composition and the amounts used for their synthesis. In all cases, the polymer was completely incorporated into the gel structure.

Table 1. Nomenclature of the Hydrogels in Relation to the Type and Amount of Polymer Used for Their Synthesis

hydrogel	polymer type (composition)	rGO/polymer weight ratio
HG1Br	MMA/BA/StBr (69/29/2)	1/0.8
HG3Br	MMA/BA/StBr (69/29/2)	1/2.4
HG1OH	MMA/BA/HEMA (49.5/49.5/1)	1/0.8
HG3OH	MMA/BA/HEMA (49.5/49.5/1)	1/2.4

The viscoelastic properties of the prepared composite hydrogels were measured and compared with those of graphene hydrogels, as shown in Figure 4. The hydrogels showed a lineal

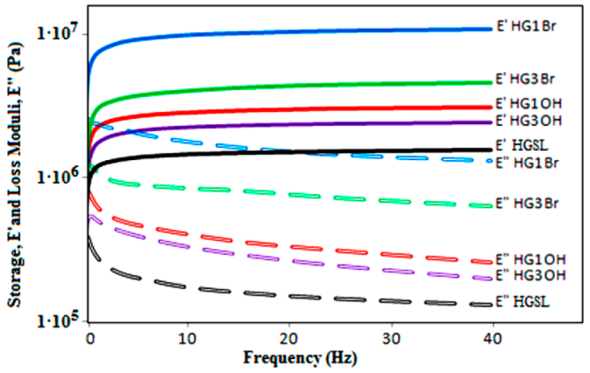

Figure 4. Comparison of the viscoelastic properties (E', storage, and E'', loss, modules) of the composite hydrogels with the neat rGO hydrogels (the nomenclature is presented in Table 1).

viscoelastic behavior in the range of 10^{-3} to 1% strain at 25 °C and 0.5 Hz. The viscosity of the hydrogels decreased greatly as they were sheared, which is a typical characteristic of self-assembled hydrogels with physical cross-links,[27] and while shearing was occurring, the rGO associations were partially broken, leading to the viscosity decrease.

In Figure 4, the storage modulus (E') and loss or viscous modulus (E'') of the hydrogels are presented as a function of the frequency. In all the studied cases, the E' value was almost 1 order of magnitude larger than the corresponding E'' value at all tested frequencies (1−100 Hz), indicating an elastic rather than a viscous response of the hydrogels under the small-deformation oscillation and thw fact that those hydrogels have a permanent network.[28]

Incorporation of the polymer into the hydrogel structure indeed improved its stiffness; thus, the storage modules at 10 rad/s improved from 2.1 × 10^6 Pa for the neat graphene hydrogel (HGSL) to 9.8 × 10^6 Pa for HG1Br. Further addition of polymer decreased the storage modules, likely because of the larger building blocks that self-organized in the hydrogel structure. For example, increasing the amount of polymer adsorbed on the platelets made the hybrid platelets larger in size; therefore, they created hydrogels with larger pores, which decreased their mechanical properties [it is demonstrated later in the morphology characterization by SEM (Figure 5)].

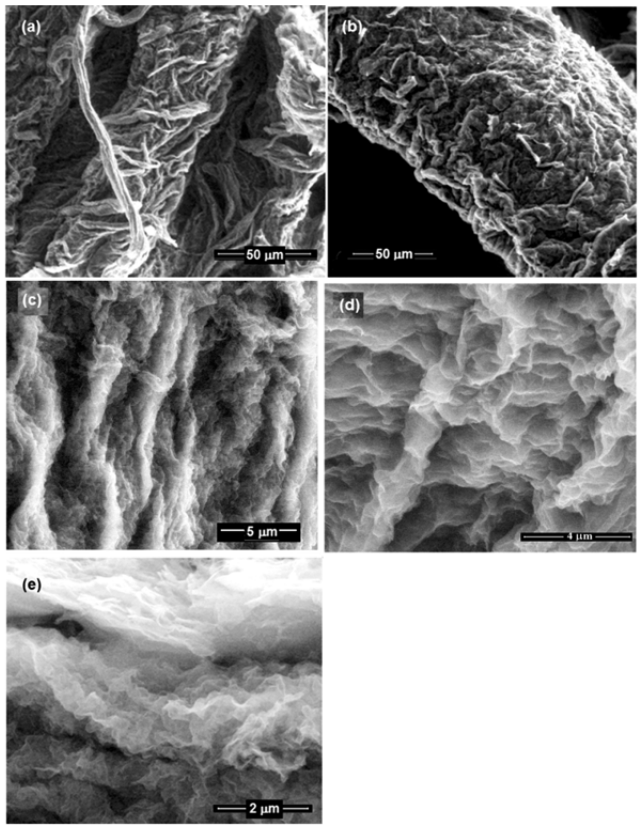

Figure 5. Morphology of the composite hydrogels: (a) HG1Br, (b, c, and e) HG3Br at different magnifications, and (d) HG3OH.

Additionally, the influence of the copolymer compositions on the mechanical properties was investigated. Hydrogels with Br functionalities had a 70/30 MMA/BA weight ratio, whereas a hydrogel with OH functionalities had a 50/50 MMA/BA weight ratio. As the content of the softer component in the copolymer (BA; T_g = −54 °C) increased, the mechanical properties significantly decreased, as shown in Figure 3. This confirms on one hand the significant dependence of the mechanical properties of the composite hydrogels on the type of incorporated polymer. On the other hand, it confirms the versatility of the proposed method and the possibility of designing tailored hydrogels for specific applications.

The morphology of the composite hydrogels investigated by SEM is presented in Figure 5 and shows twisted fibers organized in a complex hierarchical morphology, as previously demonstrated for neat graphene hydrogels.[3]

It is clear that a slight change in the procedure of the synthesis influences the self-assembly process and not only that a larger amount of polymer was included but also that the morphology was changed (in comparison to that presented in Figure 3).

Via comparison of panels a and b of Figure 5, at a lower magnification the influence of a larger amount of polymer in the structure is obvious; thus, the twisted fibers are almost 2-fold larger in diameter for the largest amount of polymer used

DOI: 10.1021/acsami.5b03325
ACS Appl. Mater. Interfaces 2015, 7, 14104−14112

[HG3Br (Figure 5b)], as the building blocks (graphene platelets decorated with polymer nanoparticles) in this case are larger. The influence of the copolymer composition on the morphology is clear from panels c and d of Figure 5; namely, the hydrogel composed of a larger amount of harder MMA polymer [HG3Br (Figure 5c)] has a structure significantly more compact than that of HG3OH (Figure 5d). This is in accordance with the better mechanical properties obtained for the former. Figure 5e at a higher magnification shows transparent crumpled hybrid platelets that created the hydrogel structure. The hierarchical porous structure of the hydrogel is clear from comparison of panels b, c, and e of Figure 5, where HG3Br is presented at an increased magnification.

Laccase Immobilization. Immobilization of laccase on the hydrogel supports occurred spontaneously at room temperature without the addition of any cross-linking reagents or additional surface modification. The principal idea was to establish physical interactions by adsorption of the laccase enzymes on the surface of the hydrogels; therefore, they were left in contact for 72 h at room temperature. However, as the immobilized laccase hydrogels (nanobiocatalysts) showed high activity after they were washed three times with 25 mM succinate buffer (pH 4.5), we hypothesized that a covalent bonding between the laccase and the support occurred. It is well-known that these buffer solutions remove physically adsorbed protein molecules from the support.[29] Besides this, the maintenance of their catalytic activity for four successive discoloration batches supports this hypothesis. Otherwise, the leaching of the enzyme from the support will result in a significant decrease in its activity from batch to batch and finally the loss of it, which was not the case. It seems that a covalent attachment was formed between the carboxyl acid groups (or other oxygen-containing groups) on the graphene oxide supports and the amine groups of the laccase enzymes.

Laccase was successfully immobilized on the hydrogel supports. Thus, immobilization yields ranging from 58.5 to 75.9% with specific activities between 7.83 and 9.47 units/mg were achieved (Table 2).

Table 2. Laccase Immobilization Yields and Specific Activities for Each Support

support	immobilization yield (%)	specific activity (units/mg)
HG1OH	58.5	7.83
HG3OH	70.0	9.29
HG1Br	65.4	8.85
HG3Br	75.9	7.89
HGSL	73.8	9.47

The immobilization yields and specific activities obtained for the composite hydrogel supports were similar to those obtained for the neat graphene hydrogel support, HGSL. This indicates that the presence of the polymer in the hydrogel structure did not affect laccase immobilization. Also, the presence of OH or Br functionalities did not affect laccase immobilization, suggesting that the polymer does not contribute to the process of immobilization.

It is worth mentioning that the immobilization of laccase on the dried forms of the composites (i.e., xerogels) failed. The reason for this could be the composition of these dried gels. During the drying process, a continuous polymeric film is formed over the rGO platelets, covering the active rGO surface (the copolymer T_g is slightly below room temperature, which allows spontaneous film formation). We speculate that the polymer is not compatible with the laccase, and this was confirmed by testing the neat polymer xerogel as a support for immobilization, which also failed. In the case of the composite hydrogels, the morphology showed nanoplatelets decorated with polymer nanoparticles that allowed the contact between the graphene and the laccase.

Stability of Immobilized and Free Laccase against Sodium Azide. The stability of both the immobilized and free laccase against the well-known laccase inhibitor sodium azide (N_3Na) was studied.

This compound inhibits laccase activity by binding to the T2/T3 site of laccase, which hampers the transfer of the electron from the T1 site to the T2/T3 site.[30,31] It was found that the free laccase lost the activity almost completely after N_3Na incubation (0.1 mM, final concentration) for 10 min (1.3%) and completely after 20 min, whereas the hydrogel-immobilized laccase kept 44.6% of activity after incubation with 0.1 mM N_3Na for 10 min and 39.3% after 20 min. Therefore, immobilization improved laccase stability against N_3Na inhibition. This is very important for the practical applications of the laccase enzymes.

Performance of the Biocatalyst. *RBBR Discoloration.* To test the applicability of the immobilized laccase, the discoloration of the anthraquinonic dye RBBR by laccase immobilized on the hydrogel supports was conducted. Three successive discoloration batches were performed. In the first batch, a dye concentration of 100 mg/L (final concentration in the flasks) was tested, and in the other two batches, a dye concentration of 200 mg/L (final concentration in the flasks) was used. The dye was added directly to the flasks as aqueous aliquots from a stock solution. In the first batch, RBBR (100 mg/L) was totally discolored in 3.5 h by all the nanobiocatalysts (Figure 6A). In the second and third batches, RBBR (200 mg/L) was almost totally discolored after 17 h by all the biocatalysts (Figure 6B,C). The increase in RBBR concentration slowed the discoloration process. The similar values attained in both batches (Figure 6B,C) showed that the nanobiocatalysts can be reutilized without losing their catalytic activity. This is very important for a cost-effective implementation of laccase enzymes on an industrial scale.

Laccase immobilized on HG3Br was also subjected to a fourth batch at a high RBBR concentration of 400 mg/L (final concentration in the flasks). It was found that the nanobiocatalyst was able to discolor the dye by 46.6% in 7 h and almost totally (91.2%) in 27 h (Figure 7). This shows the robustness of the developed nanobiocatalyst. As shown in Figure 7, the visible peak of the chromophore group (at ~600 nm) disappeared totally at the end of the laccase treatment (27 h), indicating the cleavage of the chromophore group and, thus, dye biotransformation.

It is worth mentioning that the immobilized laccase was able to discolor high concentrations (200 and even 400 mg/L) of the recalcitrant dye RBBR to a large extent with no addition of redox mediators.

As the RBBR discoloration proceeded, it could be observed that the dye solution turned from dark blue to colorless. As it is well-known that graphene hydrogels have a huge adsorption capacity,[32−34] to eliminate this possibility as a source of discoloration, a control experiment with free laccase supports was conducted. No discoloration change was detected. Also, at the end of the discoloration process, the nanobiocatalysts were immersed in methanol for 3 days to remove the presumable

DOI: 10.1021/acsami.5b03325
ACS Appl. Mater. Interfaces 2015, 7, 14104−14112

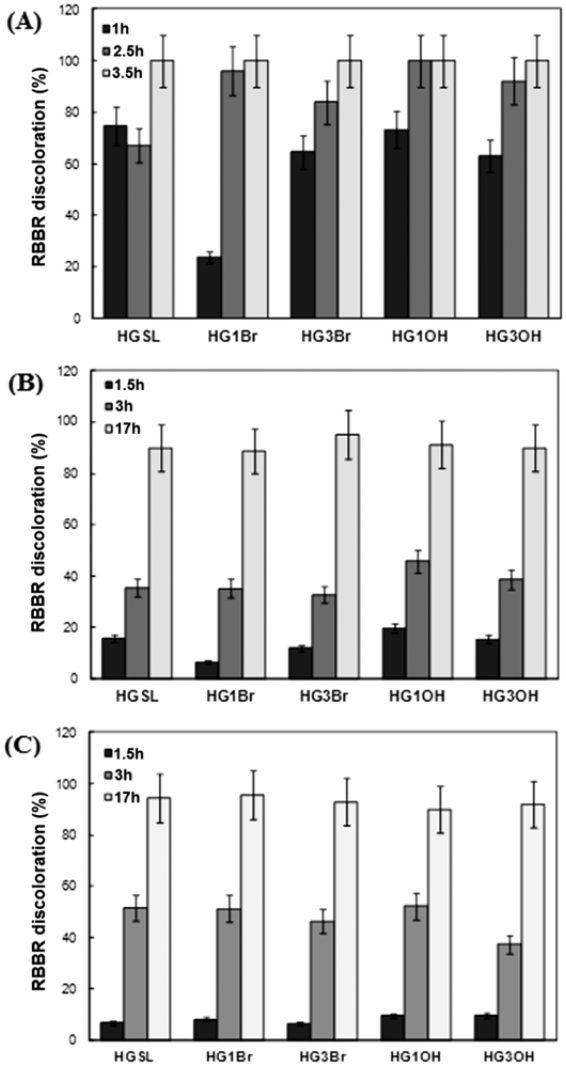

Figure 6. RBBR discoloration percentages obtained by laccase immobilized on different graphene-based hydrogel supports: (A) first batch (100 mg/L RBBR), (B) second batch (200 mg/L RBBR), and (C) third batch (200 mg/L RBBR).

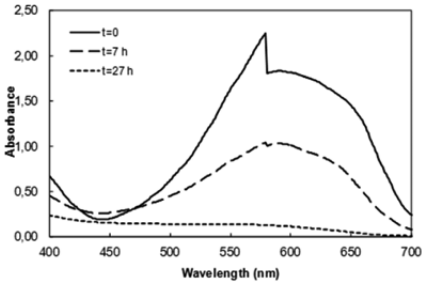

Figure 7. UV−vis spectra for the fourth batch of discoloration of RBBR by laccase immobilized on HG3Br support (400 mg/L RBBR) over time.

adsorbed dye on them. In all cases, it was found that the dye was not adsorbed on the supports, so discoloration was caused by only the action of laccase enzymes.

Determination of RBBR Biotransformation Products. To identify the metabolites of degradation of RBBR by the immobilized laccase, the original dye solution and the laccase-treated dye solution were analyzed by matrix-assisted laser desorption ionization time-of-flight mass spectrometry (MALDI-TOF MS). In Figure 8, the spectra of the initial dye solution (Figure 8a) and the final dye solution after laccase treatment (Figure 8b) are presented. Figure 8c shows magnified areas of the characteristic peaks and their assignments. Additionally, the peaks detected corresponding to different compounds are summarized in Table S2 of the Supporting Information. As a result, the metabolic pathway for the degradation of RBBR by the nanobiocatalysts was very similar to that reported previously,[33] according to which, the chromophore was broken and two subproducts were formed after laccase treatment of RBBR. The -NH_2 group of RBBR is the site for laccase attack; thus, one electron was abstracted from this group, leading to a further intramolecular rearrangement and the loss of the chromophore group of the dye. In addition, some of the obtained subproducts (Table S2 of the Supporting Information) were the same as those reported by Shatiskumar[34] for the discoloration of RBBR (50 mg/L) by a purified laccase from *Pleurotus florida*, although he obtained catechol ($C_6H_6O_2$) and anthraquinone ($C_{14}H_8O_2$) as the main transformation products.

Phytotoxicity Studies. It is also important to check the phytotoxicity of the dye before and after its transformation. In many cases following industrial processing, dye byproducts are spilled into the rivers without any treatment, posing a threat to the environment. One of the most common phytotoxicity assays used in the literature was performed by Zucconi et al.[34] This assay is applied to evaluate the phytotoxicity of plant-growing media based on the germination index (GI) of seeds. The GI combines measurements of relative seed germination and relative root elongation that are both sensitive to the presence of phytotoxic compounds. Although several species have been traditionally used for evaluating phytotoxicity, there are no standardized seed species in use worldwide.[34] In the study presented here, radish (*Raphanus sativa*) seeds were used to evaluate phytotoxicity as a representative of grasslands species, which are commonly found in the vicinity of waterways. According to Zucconi's test, values for GI of <50% mean high phytotoxicity, values between 50 and 80% mean moderate phytotoxicity, and values of >80% indicate that the material presents no phytotoxicity. GI values of 100% were obtained for all cases. Therefore, neither the dye RBBR nor its byproducts after laccase treatment were toxic.

CONCLUSIONS

Effective nanobiocatalysts, based on the enzyme laccase immobilized on the polymer/graphene hydrogel supports, were developed. The composite hydrogels were synthesized following a novel, simple, and versatile route by self-assembly of rGO platelets in a polymer latex matrix. The process of reduction of GO was used as a driving force for the self-assembly process. The versatility of the technique was proven by incorporation of a different composition of copolymers offering variation in mechanical properties of the hydrogels and different functionalities (OH and Br) offering different interactions and/or reactions with the rGO platelets, and afterward different morphologies of the hydrogels.

Immobilization of the enzyme laccase was performed in a simple way, by leaving it in contact with the hydrogels at room temperature. Even so, a covalent attachment between the enzyme and the support was formed. This resulted in highly stable and efficient nanobiocatalysts. As a proof of concept, the nanobiocatalysts were used for the degradation of the

DOI: 10.1021/acsami.5b03325
ACS Appl. Mater. Interfaces 2015, 7, 14104−14112

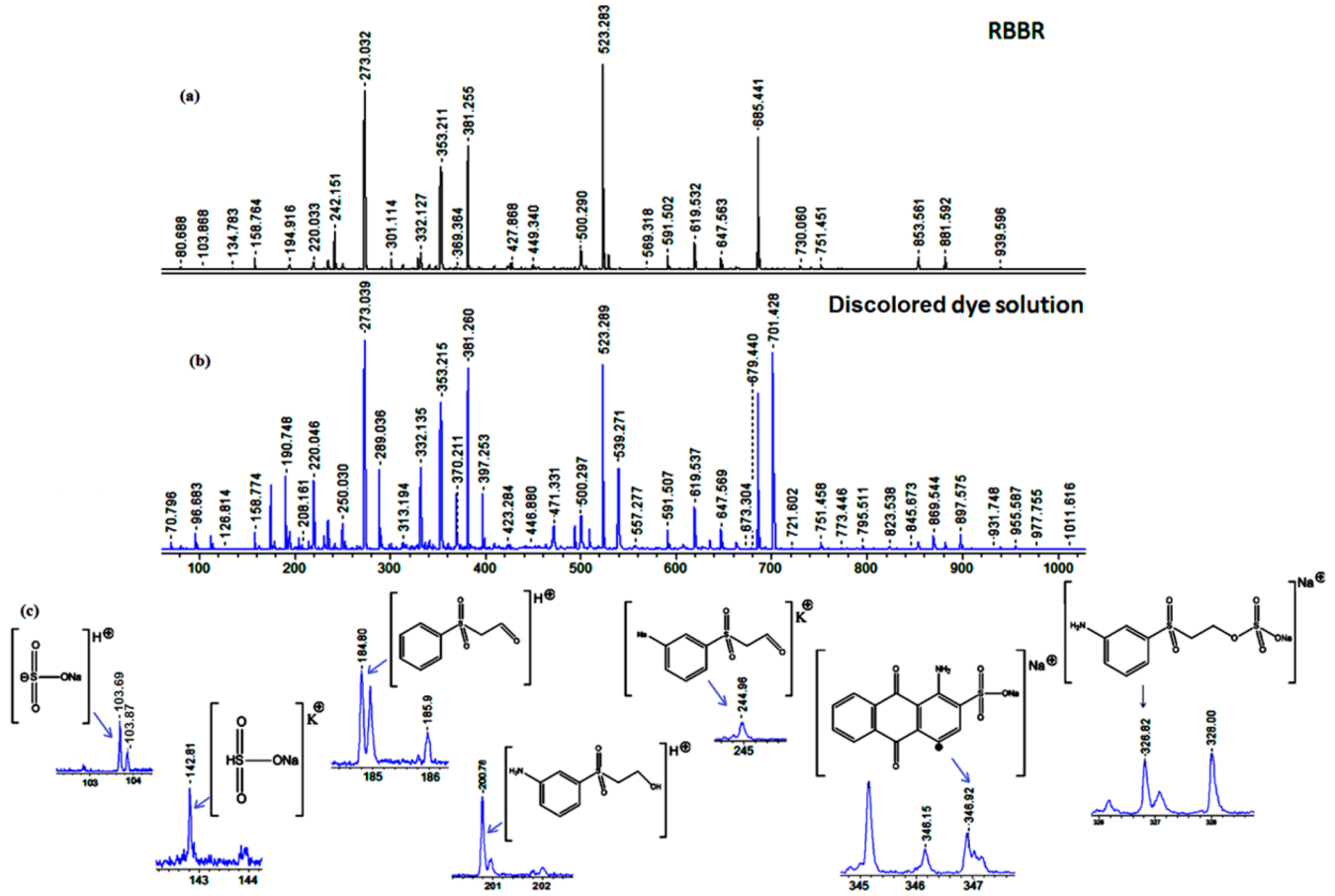

Figure 8. MALDI-TOF mass spectra of (a) RBBR and (b) the discolored dye solution in the 70−1000 Da mass range (center) obtained with DCTB and KTFA system. (c) Enlargements of the peaks accompanied by their assignments.

recalcitrant synthetic dye RBBR in aqueous solutions. The complete discoloration of relatively highly concentrated aqueous solutions of the dye was achieved in each of the four successive batches performed. This confirms that the immobilized enzyme preserved its catalytic activity and stability during the successive discoloration batches, so presumably, no leaching of the enzyme from the support occurred. These encouraging results make the use of graphene hybrid hydrogels suitable supports for laccase immobilization with potential implementation on an industrial scale. Also, they open the possibility of using the novel biocatalysts in diverse areas, such as pollution remediation, alternative energies, food industry, textile industry, pulp and paper processing, delignification for biofuels, etc.

EXPERIMENTAL SECTION

Synthesis of Hydrogels. 3D graphene/polymer composite hydrogels were formed by self-assembly of graphene oxide, GO platelets (Graphenea, concentration of 4 mg/mL, >95% monolayer content) under heating in the presence of ascorbic acid (AsA, Acros organics) as a reducing agent within the polymer latex at different ratios. Details about the synthesis of polymer latex are given in the Supporting Information. Mainly, two types of polymer nanoparticles were synthesized by seeded semicontinuous emulsion polymerization, using two different MMA/BA/functional monomer compositions in the copolymer (69/29/2 and 49.5/49.5/1). The two types of functional monomers were used 4-bromostyrene (SBr) and 2-hydroxyethyl methacrylate (HEMA). Detailed formulations are presented in the Supporting Information.

Fifty grams of the GO dispersion was mixed with latex in ratios of 1/0.8, 1/1.8, and 1/2.4, and the mixtures were stirred for 30 min with a magnetic stirrer. Afterward, AsA in various amounts (AsA/GO ratios of 0.5, 1, and 2) was added to 50 g of the GO dispersion that contained 0.2152 g GO platelets, and it was kept at 60 °C for 2 h. Composite hydrogels were formed; however, not all the amount of polymer presented in the latex was incorporated within it. In an attempt to increase the amount of polymer incorporated into the structure of the composite hydrogel, the procedure was modified and the contact between the GO and the polymer latex was increased to 3 h, before the addition of AsA. To remove residual reactants, the hydrogels were dialyzed for 1 week in ultrapure water, which controlled the conductivity until it remained constant. For that aim, a Spectral/Por dialysis membrane (Spectrumlabs) with a molecular weight cutoff of 12000−14000 Da was used. Xerogels were produced by freeze-drying of hydrogels under vacuum in a lyophilizer (Telstar LyoQuest-85).

For the characterization of hydrogels, rheology dynamic frequency experiments were performed on a Tritec 2000 DMA instrument (Triton Technology) using 10 mm × 10 mm × 2 mm samples between parallel steel plates at 25 °C in compression mode with a 2 mm gap. Frequency experiments were performed in the range of 0.4−40 Hz.

FTIR spectral analysis was conducted by measuring the hydrogel directly using an Alpha FTIR spectrophotometer Platinum ATR operated with OPUS software.

The surface morphology of the hydrogels was examined using scanning electron microscopes: a Hitachi TM3030 tabletop model at an accelerating voltage of 15 kV after the samples had been coated with a gold thin layer and a FEI Quanta 250 FEG model with low field detector (LFD) at an accelerating voltage of 10 kV under low- or high-

DOI: 10.1021/acsami.5b03325
ACS Appl. Mater. Interfaces 2015, 7, 14104−14112

vacuum mode with standard detectors. The samples were imaged after being broken under liquid nitrogen.

Laccase Immobilization. Crude laccase was immobilized on the graphene polymer-based supports synthesized as described above. The details of the crude laccase production and preparation are given in the Supporting Information.

For immobilization, 5.43 ± 0.38 g of hydrogel supports or 0.09 ± 0.03 g of xerogel supports, according to the experiment, was immersed in 15 mL of a crude laccase solution (activity of 9113 units/L; specific activity of 10.6 units/mg) for 72 h at room temperature. Afterward, the supernatant was removed and the supports were washed several times with 25 mM succinate buffer (pH 4.5) to remove the unbound laccase and protein and kept at 4 °C until further use. Bound laccase and bound protein were determined as the difference between the initial and residual laccase and protein concentrations, respectively.

Stability of Immobilized and Free Laccase against Sodium Azide. The hydrogel-immobilized laccase and the free laccase were exposed to the well-known laccase inhibitor compound sodium azide (N_3Na). For this, both laccases were incubated with 0.1 mM N_3Na in 25 mM succinic buffer at pH 4.5 for 10 and 20 min. The residual laccase activity was determined using the standard ABTS assay. Laccase activity in the absence of the inhibitor was taken to be 100%.

Performance of the Biocatalysts. The biocatalysts were used for the oxidative degradation of the synthetic dye Remazol Brilliant Blue R (RBBR) in aqueous solutions.

A stock solution of RBBR dye [1% (w/v) in water] was prepared and stored in the dark at room temperature. Dye discoloration was conducted by directly adding aliquots of this RBBR stock solution to obtain the desired concentration into 250 mL Erlenmeyer flasks containing the immobilized laccase (5.43 ± 0.38 g) and 25 mL of 25 mM succinic acid buffer (pH 4.5). Dye discoloration was performed in three successive batches. In the first batch, a dye concentration of 100 mg/L was tested, and in the other two, the dye concentration was increased to 200 mg/L. Laccase immobilized on HG3Br was also subjected to a fourth batch at a high RBBR concentration of 400 mg/L. After each batch, the nanobiocatalysts were removed from the reaction mixture by filtration, washed three times with buffer [25 mM succinic acid (pH 4.5)], and transferred into 25 mL of a fresh dye solution for the next batch. Samples were taken at the beginning of each dye addition and at determined intervals and centrifuged (8000*g* for 5 min), and the residual RBBR concentration was determined spectrophotometrically (Helios alfa, Thermo Fisher Scientific Inc.) measured from 450−500 to 700 nm and calculated by measuring the area under the plot.

For the analysis of RBBR degradation metabolites, MALDI-TOF MS measurements were performed on a Bruker Autoflex Speed system (Bruker) instrument equipped with a 355 nm NdYAG laser. All spectra were recorded in positive-ion reflectron mode. Different MALDI matrices were used: α-cyano-4-hydroxycinnamic acid (CHCA), *trans*-2-[3-(4-*tert*-butylphenyl)-2-methyl-2-propenylidene] malononitrile (DTCB), and 2-mercaptobenzothiazole (MBT). All matrices were dissolved at a concentration of 10 g/L in THF. Potassium trifluoroacetate (KTFA), sodium iodide (NaI), and sodium trifluoroacetate (NaTFA) were added as cationic ionization agents (approximately 10 g/L dissolved in THF). The matrix, salt, and polymer solutions were premixed in a 10/1/10 ratio (matrix/salt/sample). Approximately 0.5 μL of the obtained mixture was hand spotted on the ground steel target plate. For each spectrum, 5000 laser shots were recorded operating at 1 kHz. The spectra were externally calibrated using a mixture of a MW = 600 Da polyethylene glycol standard (PEG, Varian).

The toxicity of the original and the discolored dye was assessed by measuring the phytotoxicity effect of water solutions (1/3) on seed germination of radish (*Raphanus sativa*) according to the method of Zucconi et al.[30]

■ ASSOCIATED CONTENT

Supporting Information

Detailed experimental procedures and additional information about the products of biotransformation of RBBR dye, determined by MALDI-TOF MS analysis. The Supporting Information is available free of charge on the ACS Publications website at DOI: 10.1021/acsami.5b03325.

■ AUTHOR INFORMATION

Corresponding Authors

*E-mail: radmila.tomovska@ehu.es.
*E-mail: srodriguez@ceit.es.

Notes

The authors declare no competing financial interest.

■ ACKNOWLEDGMENTS

The financial support of the Basque Government (GV IT373-10 and IE14-393), NATO (SfP 984399), Diputacion Foral de Gipuzkoa (Exp. 55/14), and University of the Basque Country UPV/EHU (UFI11/56) is gratefully acknowledged.

■ ABBREVIATIONS

GO, graphene oxide; rGO, reduced graphene oxide; MMA, methyl methacrylate; BA, butyl acrylate; HEMA, hydroxyethyl methacrylate; SBr, 3-bromostyrene

■ REFERENCES

(1) Pavlidis, I. V.; Patila, M.; Bornscheuer, U. T.; Gournis, D.; Stamatis, H. Graphene-Based Nanobiocatalytic Systems: Recent Advances and Future Prospects. *Trends Biotechnol.* **2014**, *32*, 312−320.
(2) Tran, D. N.; Balkus, K. J. Perspective of Recent Progress in Immobilization of Enzymes. *ACS Catal.* **2011**, *1*, 956−968.
(3) Rodriguez-Couto, S.; Arzac, A.; Leal, G. P.; Tomovska, R. Reduced Graphene Oxide Hydrogels and Xerogels Provide Efficient Platforms for Immobilization and Laccase Production by Trametes Pubescens. *Biotechnol. J.* **2014**, *9*, 578−584.
(4) Gaharwar, A. K.; Peppas, N. A.; Khademhosseini, A. Nanocomposite Hydrogels for Biomedical Applications. *Biotechnol. Bioeng.* **2014**, *111*, 441−453.
(5) Lo, C. W.; Zhu, D.; Jiang, H. An Infrared-Light Responsive Graphene-Oxide Incorporated Poly(N-isopropylacrylamide) Hydrogel Nanocomposite. *Soft Matter* **2011**, *7*, 5604−5609.
(6) Singh, R.; Tiwari, M.; Singh, R.; Lee, J. K. From Protein Engineering to Immobilization: Promising Strategies for the Upgrade of Industrial Enzymes. *Int. J. Mol. Sci.* **2013**, *14*, 1232−1277.
(7) Sheng, K. X.; Xu, Y. X.; Li, C.; Shi, G. Q. High-Performance Self-Assembled Graphene Hydrogels Prepared by Chemical Reduction of Graphene Oxide. *New Carbon Materials* **2011**, *26*, 9−15.
(8) Chen, W.; Yan, L. In Situ Self-Assembly of Mild Chemical Reduction Graphene for Three-Dimensional Architectures. *Nanoscale* **2011**, *3*, 3132−3137.
(9) Rodríguez Couto, S.; Toca Herrera, J. L. Industrial and Biotechnological Applications of Laccases: A Review. *Biotechnol. Adv.* **2006**, *24*, 500−513.
(10) Brady, D.; Jordaan, J. Advances in Enzyme Immobilisation. *Biotechnol. Lett.* **2009**, *31*, 1639−1650.
(11) Guzik, U.; Hupert-Kocurek, K.; Wojcieszynska, D. Immobilization as a Strategy for Improving Enzyme Properties: Application to Oxidoreductases. *Molecules* **2014**, *19*, 8995−9018.
(12) Chen, W.; Li, S.; Chen, C.; Yan, L. Self-Assembly and Embedding of Nanoparticles by In Situ Reduced Graphene for Preparation of a 3D Graphene/Nanoparticle Aerogel. *Adv. Mater. (Weinheim, Ger.)* **2011**, *23*, 5679−5683.

DOI: 10.1021/acsami.5b03325
ACS Appl. Mater. Interfaces 2015, 7, 14104−14112

(13) Chandra, V.; Kim, K. S. Highly Selective Adsorption of Hg^{2+} by a Polypyrrole-Reduced Graphene Oxide Composite. *Chem. Commun.* **2011**, *47*, 3942−3944.
(14) Qiu, L.; Liu, D.; Wang, Y.; Cheng, C.; Zhou, K.; Ding, J.; Truong, V.-T.; Li, D. Mechanically Robust, Electrically Conductive and Stimuli-Responsive Binary Network Hydrogels Enabled by Superelastic Graphene Aerogels. *Adv. Mater. (Weinheim, Ger.)* **2014**, *26*, 3333−3337.
(15) Vickery, J. L.; Patil, A. J.; Mann, S. Fabrication of Graphene−Polymer Nanocomposites with Higher-Order Three-Dimensional Architectures. *Adv. Mater. (Weinheim, Ger.)* **2009**, *21*, 2180−2184.
(16) Chandra, V.; Yu, S. U.; Kim, S. H.; Yoon, Y. S.; Kim, D. Y.; Kwon, A. H.; Meyyappan, M.; Kim, K. S. Highly Selective CO_2 Capture on N-Doped Carbon Produced by Chemical Activation of Polypyrrole Functionalized Graphene Sheets. *Chem. Commun.* **2012**, *48*, 735−737.
(17) Sahu, A.; Choi, W. I.; Tae, G. A Stimuli-Sensitive Injectable Graphene Oxide Composite Hydrogel. *Chem. Commun.* **2012**, *48*, 5820−5822.
(18) Ren, L.; Huang, S.; Fan, W.; Liu, T. One-Step Preparation of Hierarchical Superparamagnetic Iron Oxide/Graphene Composites via Hydrothermal Method. *Appl. Surf. Sci.* **2011**, *258*, 1132−1138.
(19) Liu, J.; Cui, L.; Kong, N.; Barrow, C. J.; Yang, W. RAFT Controlled Synthesis of Graphene/Polymer Hydrogel with Enhanced Mechanical Property for pH-Controlled Drug Release. *Eur. Polym. J.* **2014**, *50*, 9−17.
(20) Li, W.; Wang, J.; Ren, J.; Qu, X. 3D Graphene Oxide−Polymer Hydrogel: Near-Infrared Light-Triggered Active Scaffold for Reversible Cell Capture and On-Demand Release. *Adv. Mater. (Weinheim, Ger.)* **2013**, *25*, 6737−6743.
(21) Bai, H.; Sheng, K.; Zhang, P.; Li, C.; Shi, G. Graphene Oxide/Conducting Polymer Composite Hydrogels. *J. Mater. Chem.* **2011**, *21*, 18653−18658.
(22) Wang, Y.; Chen, S.; Qiu, L.; Wang, K.; Wang, H.; Simon, G. P.; Li, D. Graphene-Directed Supramolecular Assembly of Multifunctional Polymer Hydrogel Membranes. *Adv. Funct. Mater.* **2015**, *25*, 126−133.
(23) Liu, J.; Chen, G.; Jiang, M. Supramolecular Hybrid Hydrogels from Noncovalently Functionalized Graphene with Block Copolymers. *Macromolecules* **2011**, *44*, 7682−7691.
(24) Banerjee, S.; Das, R. K.; Maitra, U. Supramolecular Gels 'In Action'. *J. Mater. Chem.* **2009**, *19*, 6649−6687.
(25) Sangeetha, N. M.; Maitra, U. Supramolecular Gels: Functions and Uses. *Chem. Soc. Rev.* **2005**, *34*, 821−836.
(26) Preston, T. C.; Nuruzzaman, M.; Jones, N. D.; Mittler, S. Role of Hydrogen Bonding in the pH-Dependent Aggregation of Colloidal Gold Particles Bearing Solution-Facing Carboxylic Acid Groups. *J. Phys. Chem. C* **2009**, *113*, 14236−14244.
(27) Chen, G. H.; Hoffman, A. S. Graft Copolymers that Exhibit Temperature-Induced Phase-Transitions Over a Wide Range of pH. *Nature* **1995**, *373*, 49−52.
(28) Xu, Y.; Sheng, K.; Li, C.; Shi, G. Self-Assembled Graphene Hydrogel via a One-Step Hydrothermal Process. *ACS Nano* **2010**, *4*, 4324−4330.
(29) Liu, Y.; Li, Q.; Feng, Y.-Y.; Ji, G.-S.; Li, T.-C.; Tu, J.; Gu, X.-D. Immobilisation of Acid Pectinase on Graphene Oxide Nanosheets. *Chem. Pap.* **2014**, *68*, 732−738.
(30) Gianfreda, L.; Xu, F.; Bollag, J.-M. Laccases: A Useful Group of Oxidoreductive Enzymes. *Biorem. J.* **1999**, *3*, 1−26.
(31) Xu, F. Oxidation of Phenols, Anilines, and Benzenethiols by Fungal Laccases: Correlation between Activity and Redox Potentials as Well as Halide Inhibition. *Biochemistry* **1996**, *35*, 7608−7614.
(32) Zhao, W.; Tang, Y.; Xi, J.; Kong, J. Functionalized Graphene Sheets with Poly(Ionic Liquid)s and High Adsorption Capacity of Anionic Dyes. *Appl. Surf. Sci.* **2015**, *326*, 276−284.
(33) Kim, H.; Kang, S. O.; Park, S.; Park, H. S. Adsorption Isotherms and Kinetics of Cationic and Anionic Dyes on Three-Dimensional Reduced Graphene Oxide Macrostructure. *J. Ind. Eng. Chem.* **2015**, *21*, 1191−1196.
(34) Wu, Z.; Zhong, H.; Yuan, X.; Wang, H.; Wang, L.; Chen, X.; Zeng, G.; Wu, Y. Adsorptive Removal of Methylene Blue by Rhamnolipid-Functionalized Graphene Oxide from Wastewater. *Water Res.* **2014**, *67*, 330−344.

DOI: 10.1021/acsami.5b03325
ACS Appl. Mater. Interfaces 2015, 7, 14104−14112